J|A|C|S
ARTICLES
Published on Web 04/18/2002

Close-Packed C_{70}^{3-} Phases − Synthesis, Structure, and Electronic Properties

Mark S. Denning,[†] Ian D. Watts,[‡] Sandra M. Moussa,[‡] Pierrick Durand, Matthew J. Rosseinsky,*[,‡] and Katsumi Tanigaki[§]

Contribution from the Inorganic Chemistry Laboratory, Department of Chemistry, University of Oxford, South Parks Road, Oxford OX1 3QR, U.K., Department of Chemistry, University of Liverpool, Liverpool, L69 7ZD, U.K., Department of Materials Science, Faculty of Science, Osaka City University, and CREST, JST, 3-3-138 Sugimoto, Sumiyoshi-ku, Osaka 558-8585, Japan

Received December 17, 2001

Abstract: The high symmetry and resulting electronic degeneracy of the C_{60}^{3-} anion is viewed as the key molecular feature in the high superconducting transition temperatures of fulleride and oxidized fullerene systems. The experimental evaluation of this hypothesis requires the synthesis of face-centered cubic (fcc) trivalent fulleride anion salts derived from higher fullerenes such as C_{70}, which have thus far proved elusive with only stable A_1C_{70}, A_4C_{70}, and A_6C_{70} phases known. In this paper, we report the synthesis of fcc A_3C_{70} phases stabilized by size-matching the tetrahedral site with the sodium cation. The structures are strongly dependent on the cooling protocol due to the existence of metastable partially or completely orientationally disordered phases. EPR data indicate that the phases are metallic but not superconducting. The densities of states at the Fermi level appear too low to give superconductivity at above 5 K, consistent with recent observations that four electrons per C_{70} anion are required for superconductivity. Size-matching on both the octahedral and tetrahedral sites is required for A_3C_{70} stability − K_2CsC_{70} is only stable at elevated temperature and Na_2C_{70} is unstable, the composition corresponding to C_{70} and a sodium-rich trigonal phase.

Introduction

The A_3C_{60} alkali metal fullerides have superconducting transition temperatures exceeded only by the copper oxides;[1,2] oxidation of expanded C_{60} phases affords a transition temperature of 117 K.[3] Although a precise theoretical description of the normal and superconducting states is still lacking, the high degeneracy of the C_{60} frontier orbitals arising from the I_h point symmetry and the half-filled band arising from the $(t_{1u})^3$ configuration of the C_{60}^{3-} anion appear to be key chemical features. An important chemical test of this idea would be the synthesis of fcc A_3C_n phases derived from higher C_n fullerenes of lower-point symmetry than C_{60}. The most abundant higher fullerene, C_{70}, is appropriate as its D_{5h} point symmetry affords a singly degenerate LUMO, slightly lower in energy than the doubly degenerate (LUMO + 1) level (Figure 1a);[4] the threefold orbital degeneracy of the t_{1u} C_{60} LUMO is not allowed in the C_{70} point group. The elongated ellipsoidal shape of C_{70} is derived from that of C_{60} by adding a ring of 10 carbon atoms around the equatorial plane of the C_{60} molecule, and gives a wide variety of temperature-dependent structural phases[5] due to the successive freezing-out of reorientations of the molecule about its different symmetry directions. The nonspherical nature of C_{70} has however made the synthesis of fcc A_3C_{70} analogues, containing C_{70}^{3-} anions,[6] difficult. For example, K_3C_{70} is reported only to be stable above 440 K, disproportionating into K_1C_{70}[7] and K_4C_{70} below this temperature. A metallic K_4C_{70} phase,[8] together with insulating $x = 1$, 6, and 9 phases have been reported.[9] Sm_3C_{70} is an fcc C_{70}^{6-} phase.[10] Given the observation of superconductivity in C_{70} field-effect transistors[11] at a doping level of four electrons per molecule, corresponding to a half-filled (LUMO + 1) band, the synthesis of nonsuperconducting C_{70}^{3-} salts would indicate the strong connection between the half-filled band and superconductivity in fulleride systems.

Consideration of the radii of the tetrahedral (1.18 Å) and octahedral (2.17 Å) holes in fcc C_{70} in comparison to the ionic radii of the alkali metals (Cs^+ − 1.7 Å, Rb^+ − 1.5 Å, K^+ −

* To whom correspondence should be addressed. E-mail: m.j.rosseinsky@liv.ac.uk.
[†] Department of Chemistry, University of Oxford.
[‡] Department of Chemistry, University of Liverpool.
[§] Department of Materials Science, Osaka City University.

(1) Rosseinsky, M. J. *Chem. Mater.* **1998**, *10*, 2665−2685.
(2) Prassides, K. *Curr. Opin. Solid State Mater. Sci.* **1997**, *2*, 433−439.
(3) Schon, J. H.; Kloc, C.; Batlogg, B. *Science* **2001**, *293*, 2432−2434.
(4) Nakao, K.; Kurita, N.; Fujita, M. *Phys. Rev. B* **1994**, *49*, 11415.
(5) Vaughan, G. B. M.; Heiney, P. A.; Cox, D. E.; Fischer, J. E.; McGhie, A. R.; Smith, A. L.; Strongin, R. M.; Cishy, M. A.; Smith, A. B., III. *Chem. Phys.* **1993**, *178*, 599−613.
(6) Saito, S.; Cohen, M. L. *Solid State Comm.* **1996**, *99*, 891−896.
(7) Knupfer, M.; Poirier, D. M.; Weaver, J. H. *Phys. Rev. B* **1994**, *49*, 8464−8473.
(8) Wang, Z. H.; Dresselhaus, M. S.; Dresselhaus, G.; Eklund, P. C. *Phys. Rev. B* **1993**, *48*, 16881−16884.
(9) Kobayashi, M.; Akahama, Y.; Kawamura, H.; Shinohara, H.; Sato, H.; Saito, Y. *Phys. Rev. B* **1993**, *48*, 16877−16880.
(10) Chen, X. H.; Chi, D. H.; Sun, Z.; Takenobu, T.; Liu, Z. S.; Iwasa, Y. *J. Amer. Chem. Soc.* **2000**, *122*, 5729−5732.
(11) Schon, J. H.; Kloc, C.; Siegrist, T.; Steigerwald, M.; Svensson, C.; Batlogg, B. *Nature* **2001**, *413*, 831−833.

10.1021/ja017780b CCC: $22.00

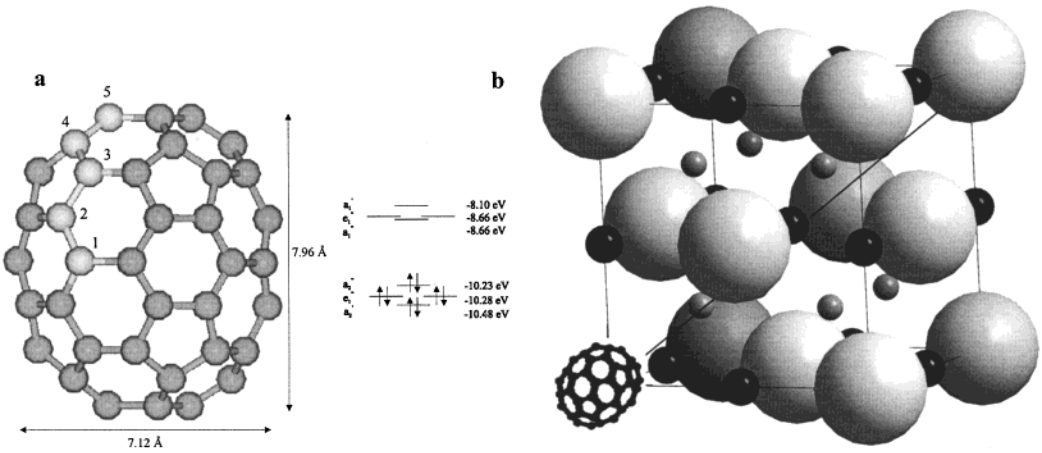

Figure 1. (a) The C_{70} molecule, indicating the five distinct carbon atoms, with a representation of the frontier molecular orbitals. (b) The target A_3C_{70} fcc structure. The size of the cations suitable to occupy the O (small black spheres) and T (small dark gray spheres) sites can be estimated from the spherical shell site sizes, and the size of the O site is sufficient to accommodate tetrahedral and cubic groups of cations. The [111] body diagonal is shown and orientation of the long axis of the C_{70} molecule with this direction would produce rhombohedral symmetry.

1.3 Å, Na^+ − 0.95 Å) shows only tetrahedral sodium is small enough not to interfere with the isotropic free rotation of the C_{70} molecule (Figure 1b). It follows that Na_2AC_{70} salts are the most promising candidates for the preparation of a metastable cubic A_3C_{70} phase. The large Cs^+ cation appears to have the best size match with the octahedral site. The experiments described in this paper are designed to test the influence of the size of both octahedral and tetrahedral cations on the stability of the A_3C_{70} phases. The resulting synthesis of Na_2CsC_{70} with a variety of orientational orderings of the C_{70}^{3-} anions allows the investigation of the electronic and dynamical properties of these phases, which indicate that metallic but not superconducting behavior is possible at the C_{70}^{3-} composition. To determine the importance of size-matching on the octahedral and tetrahedral sites, we investigated the synthesis of the octahedral cation-free Na_2C_{70} (in the Na_2C_{60} salt the Na^+ cations occupy solely the tetrahedral sites) and K_2CsC_{70}, in which larger cations occupy the tetrahedral site. Each system behaves in a distinctive manner, indicating the importance of size -matching on both sites to the observed chemistry.

Experimental Section

Synthesis. Inside a helium-filled Mbraun Labmaster glovebox, stoichiometric quantities of sublimed C_{70} (typically 100 mg) and alkali metals were weighed into a stainless steel tube, which was then placed inside a 9-mm OD Pyrex tube and sealed off at 2×10^{-4} Torr. Reactions were also performed with stoichiometric quantities of reagents sealed under argon in arc-welded tantalum tubes. The reaction vessel was then placed in a tube furnace and the sample heated for one day at each of the following temperatures: 200 °C, 250 °C, 300 °C, 350 °C. The samples were then reground and a final heating stage at a temperature of at least 450 °C was undertaken, with different cooling procedures (quenching into oil, cooling by removal from the furnace, cooling at rates of between 0.1 and 0.01 °C min^{-1}) being adopted and specified for each sample when it is discussed. The range of cooling procedures was adopted due to the well-documented dependence of the structures of pristine C_{70} on thermal history.[12] These samples were then characterized using the following physical techniques.

X-ray Powder Diffraction. Initial characterization was accomplished using Siemens D5000 and Stoe STADI−P diffractometers in transmission geometry (Cu $K\alpha_1$ radiation, linear position sensitive detectors) with the samples sealed under helium in Lindemann capillary tubes. Synchrotron powder X-ray diffraction data were recorded on the BM16 diffractometer at the ESRF, Grenoble ($\lambda = 0.850747(1)$ Å) and at station 9.1 at the Synchrotron Radiation Source, Daresbury Laboratory, UK ($\lambda = 0.99871(1)$ Å) at both room temperature and in hot air blower (ESRF) or furnace (DL) environments at temperatures up to 400 °C. For the high-temperature experiments the samples were sealed under helium in thin-walled quartz capillaries. Analysis of the X-ray powder diffraction data was performed with the GSAS[13] and Fullprof[14] Rietveld refinement software. The X-ray form factor, $f_{mol}(q)$, of the C_{70} molecule was calculated from eq 1

$$f_{mol}(q) = f_C(q)\sum_{i=1}^{5} N_i \frac{\sin(qR_i)}{qR_i} \qquad (1)$$

where $f_C(q)$ is the scattering factor of a carbon atom and is a function of the momentum transfer q; N_i is the number of carbon atoms at a radius R_i (Figure S1, Supplementary Information). This molecular form factor is appropriate for an isotropically tumbling C_{70} molecule, based on five concentric spheres of scattering density from the five independent carbon atoms.

Magic Angle Spinning (MAS) NMR Spectroscopy. Data were collected using a CMX Infinity spectrometer at 50.3 MHz (4.7 T) with the sample (≈100 mg) sealed in a precision ground glass ampule and spun in a Chemagnetics 7.5 mm OD zirconia rotor. Adamantane was used as a ^{13}C secondary standard. Spectra were recorded at variable spinning speeds of up to 6 kHz at temperatures between 25 and 250 °C.

EPR Spectroscopy. EPR data were collected using a Varian E-line spectrometer at a microwave frequency of 9.23 GHz between 5 and 300 K: g-values were calibrated with a DPPH standard and the magnetic susceptibility was calibrated using K_3C_{60}, whose susceptibility was taken to be 8.5×10^{-4} emu mol^{-1}.[15] The power dependence of the EPR signals was checked in all cases at 5 K to avoid saturation of any of the signals reported. The powers used to record spectra varied between 0.01 and 0.4 mW.

Raman Spectroscopy. Raman measurements were carried out using a Dilor LABRAM spectrometer with a HeNe laser at 10 W/cm^2 power density with a wavelength of 632.817 nm. The power density was

(12) Christides, C.; Thomas, I. M.; Dennis, T. J. S.; Prassides, K. *Europhys. Lett.* **1993**, *22*, 611−618.

(13) Larson, A. C.; von Dreele, R. B. *General Structure Analysis System;* Los Alamos National Laboratory: Los Alamos, 1994.

(14) Rodriguez-Carvajal, J. *Fullprof*; 3.5 ed.; Institut Laue-Langevin, 1998.

(15) Wong, W. H.; Hanson, M. E.; Clark, W. G.; Gruner, G.; Thompson, J. D.; Whetten, R. L.; Huang, S.-M.; Kaner, R. B.; Diederich, F.; Petit, P.; Andre, J.-J.; K Holczer *Europhys. Lett.* **1992**, *18*, 79−84.

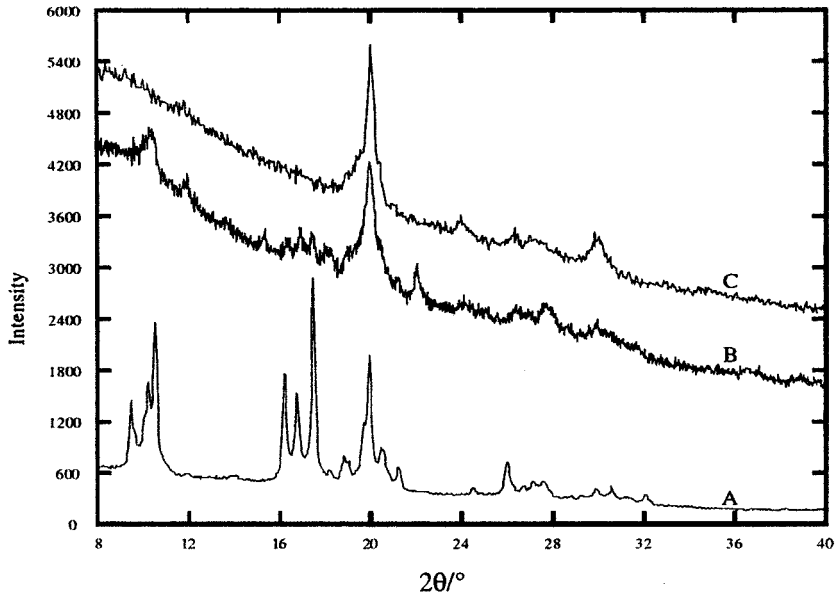

Figure 2. Evolution of the powder X-ray diffraction pattern during the preparation of Na_2CsC_{70} at stages described in the text.

selected to avoid polymerization of the C_{70} anions which manifested itself as time-dependence of spectra recorded at higher powers.

SQUID Magnetometry. D.c. magnetization measurements were performed using a Quantum Design MPMS-7T SQUID magnetometer over the range $1.5 \leq T/K \leq 30$ in a 10 Oe field to search for superconductivity.

Results

Na_2CsC_{70}. Figure 2 illustrates the laboratory X-ray powder diffraction patterns of the C_{70} starting material (A) and the Na_2CsC_{70} composition after the initial heat treatment (final temperature 350 °C) (B) and subsequent reaction at 450 °C (C). These data show that unreacted C_{70} is present after reaction at 350 °C, so the higher reaction temperatures were used throughout the study. The subsequent thermal treatment, particularly the cooling protocol, makes a difference to the detailed behavior (anion orientational ordering, cation location and displacement parameters) but the overall features of the diffraction patterns of the four Na_2CsC_{70} samples discussed below are similar.

Simple removal of the sample from the furnace after three days at 450 °C produced sample I. Although the X-ray intensity distribution resembled that expected for an fcc Na_2CsC_{70} phase with a lattice parameter of approximately 14.65 Å, detailed inspection of the synchrotron X-ray powder diffraction pattern indicated that each of the fundamental fcc reflections was split into several heavily overlapping contributing reflections (Figure S2). Attempts to assign a unit cell using autoindexing programs were unsuccessful, and it was concluded that this procedure led to an assembly of several fcc or lower symmetry phases, related to fcc by anion orientational ordering. Attention was therefore paid to the thermal treatment of the sample on cooling from the reaction temperature.

Sample II was prepared by a final heating at 600 °C followed by quenching to room temperature in oil. The main features of this diffraction pattern can be indexed on the basis of a fcc unit cell with $a = 14.75$ Å. However, the variation of the peak width with angle is nonphysical for a single fcc phase, strongly suggesting that although the crystal structure is based on fcc packing of the C_{70}^{3-} anions, there is a symmetry lowering induced by orientational ordering of the anions. Indexing and Lebail extraction of the data indicated the space group $C2/m$ ($\chi^2 = 5.43$, Figure S3a) $a = 18.19(1)$ Å, $b = 10.406(7)$ Å, $c = 14.86(1)$ Å, and $\beta = 144.78(7)°$, consistent with orientational ordering transitions producing symmetry lowering from cubic first to rhombohedral and then to monoclinic. The relationship between the rhombohedral and monoclinic unit cells is given in Figure S3b. It is important to note that monoclinic symmetry is required in C_{70} compounds if the anions are to be completely orientationally ordered. Rietveld refinement of the data was performed using the approximation (1) for the C_{70} form factor (there are insufficient data to allow the refinement of the molecular geometry) with the refined pattern ($\chi^2 = 6.48$) shown in Figure 3a and the refined parameters given in Table 1. The refined composition of $Na_{2.04(8)}Cs_{1.068(8)}C_{70}$ corresponds well to the nominal composition, although the displacement parameters are comparable to those refined at higher temperatures (vide infra) and indicate considerable cation disorder. Another possible explanation for the complexity of the observed diffraction pattern is the presence of more than one phase. With this in mind, a two-phase refinement was performed using rhombohedral and cubic phases. The rhombohedral phase is derived from the cubic phase by a deformation along the [111] direction of the cubic unit cell and would arise from preferential alignment of the long axis of the ellipsoidal C_{70} molecule with this body diagonal. This model provided a better fit to the data than any of the single-phase models ($\chi^2 = 5.54$, Figure 3b). The atomic parameters, for both phases, are summarized in Table 2. Given the breadth of the diffraction maxima, it is impossible to differentiate between the monoclinic and mixed cubic/rhombohedral models, but it is clear that there is at least partial orientational ordering of the anions at room temperature.

Sample III was prepared by slow cooling (0.1 °C min^{-1}) from the final reaction temperature of 450 °C, with the resulting room temperature diffraction pattern being consistent with a two-phase mixture or monoclinic symmetry as found for sample II above. This complex broad pattern changed drastically on heating (Figure 4a), with the reflections in the region of the cubic 311

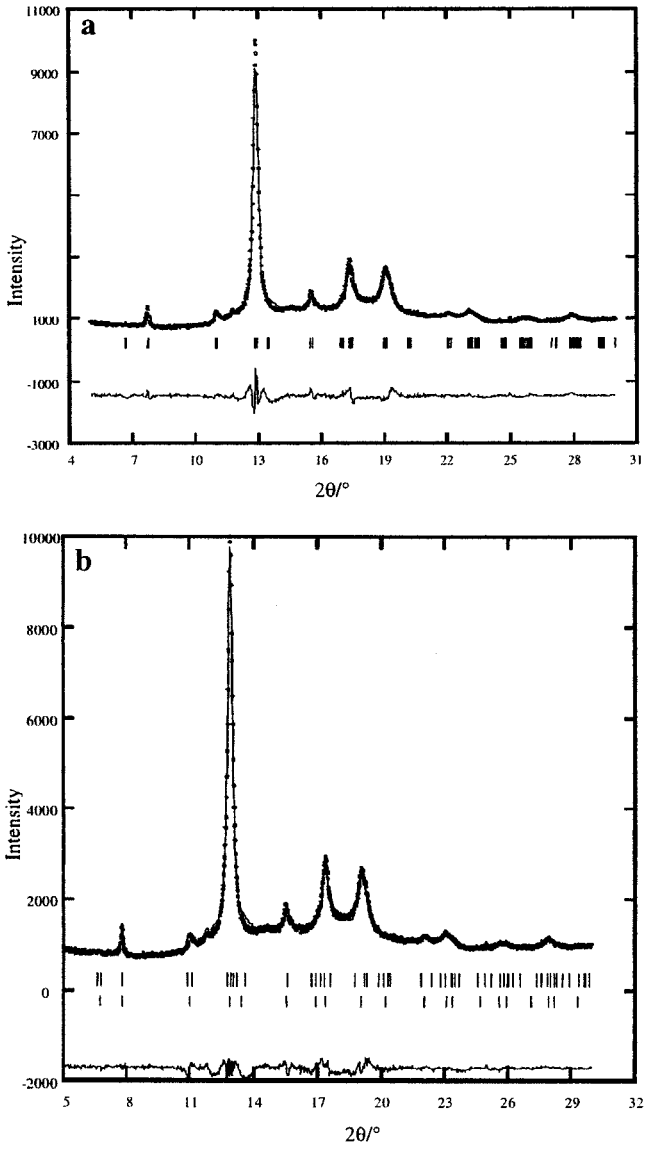

Figure 3. (a) Rietveld refinement of room-temperature synchrotron X-ray data from Na_2CsC_{70} quenched from 600 °C (sample II) data in space group *C*2/*m*. The observed data are shown as points, the calculated fit is the solid line and the difference curve is plotted below. The tick marks indicate the positions of the allowed Bragg reflections. (b) Refinement of room-temperature synchrotron X-ray data from Na_2CsC_{70} quenched from 600 °C with a two-phase ($R\bar{3}m$ (upper ticks) and $Fm\bar{3}m$ (lower ticks)) model.

Table 1. Refined Parameters for Na_2CsC_{70} (Sample II) at Room Temperature[a]

	x	*y*	*z*	B_{iso}/Å^2	fractional occupancy
C_{70}	0.0	0.0	0.0	2.6(7)	1.000
Na	0.0	0.5	0.303(5)	21.7(1)	1.02(4)
Cs	0.0	0.0	0.5	26.4(7)	1.068(8)

[a] *C*2/*m* a = 18.19(1) Å, b = 10.406(7) Å, c = 14.86(1) Å, and β = 144.78(7)°, χ^2 = 6.48, R_{wp} = 4.1%, $R(F^2)$ = 9.27%.

reflection expected to be most intense for Na_2CsC_{70} sharpening dramatically on heating above 100 °C. The sharp reflections seen at 250 °C indicate that a phase transition has occurred on heating, and this is confirmed by quantitative analysis of the data. Data recorded on cooling (Figure 4b) indicate that these sharp reflections are maintained at room temperature, indicating considerable thermal hysteresis and the supercooling of a metastable high-symmetry phase. (Figure S4a shows the full

Table 2. Refined Parameters from the Constrained Two-phase Refinement of Na_2CsC_{70} (Sample II)[a]

	x	*y*	*z*	B_{iso}/Å^2	fractional occupancy
$Fm\bar{3}m$ Phase (a = 14.804(5) Å) − 3.18%					
C_{70}	0.0	0.0	0.0	−0.1(9)	1
Na	0.25	0.25	0.25	33(2)	1.12(4)
Cs	0.5	0.5	0.5	26.8(8)	1.09(2)
$R\bar{3}m$ Phase (a = b = 10.32(1) Å, c = 26.11(2) Å) − 96.82%					
C_{70}	0.0	0.0	0.0	−0.1(9)	1
Na	0	0	0.214(3)	33(2)	1.12(4)
Cs	0.0	0.0	0.5	26.8(8)	1.09(2)

[a] The model includes a majority rhombohedral phase and a minority cubic phase; χ^2 = 5.54, R_{wp} = 3.65%.

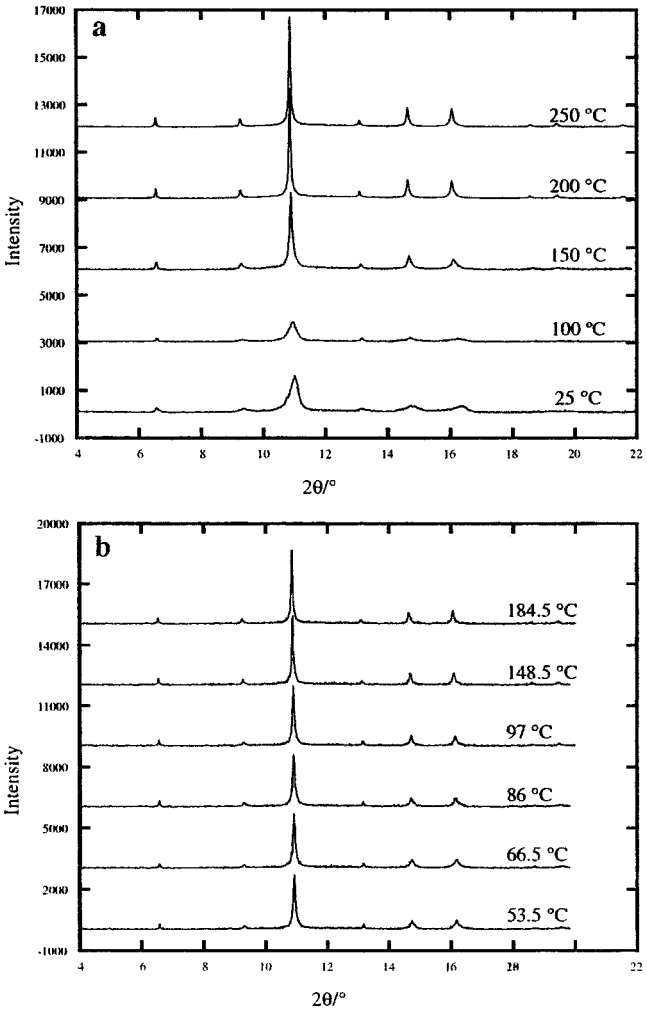

Figure 4. (a) Evolution of the synchrotron X-ray powder diffraction pattern of Na_2CsC_{70} (sample III) on heating to 250 °C. (b) Evolution of the diffraction pattern of Na_2CsC_{70} (sample III) on cooling from 250 °C.

width at half-maximum for all the observed reflections on heating and cooling.) The difference in comparison with the bulk samples above can be assigned to the small thermal mass of the capillary.

Following identification of the transition temperature, the sample was reheated into the cubic region and data for Rietveld refinement were collected at 350 °C for 8 h − the diffraction pattern of the sample did not change over this period. Le Bail extraction indicates that the sample is metrically cubic rather than rhombohedral (the refined rhombohedral cell parameters are less than three standard deviations away from the cubic

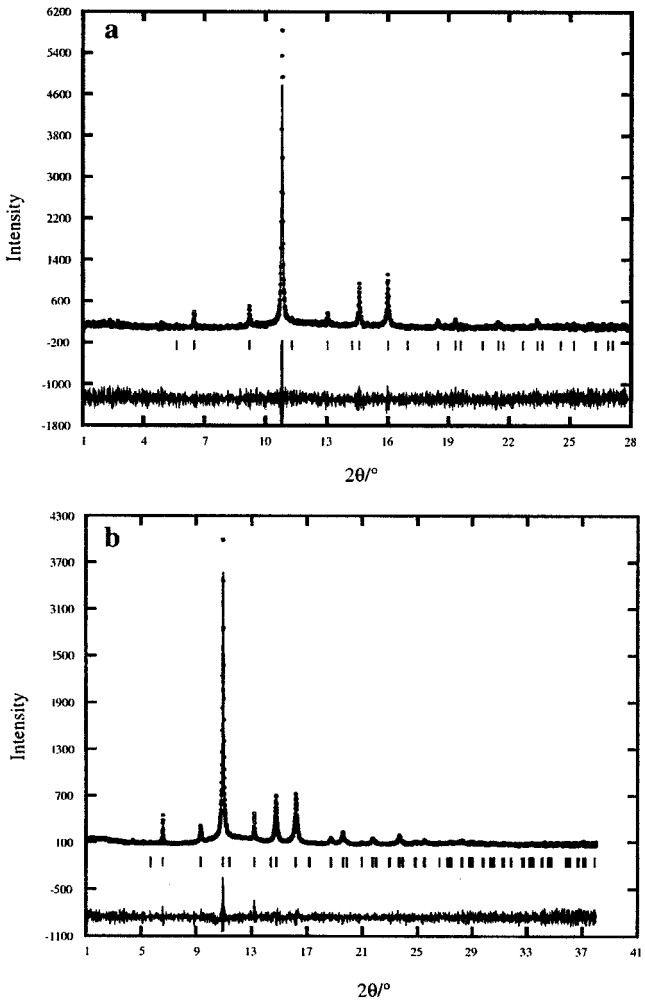

Figure 5. (a) Rietveld refinement of Na_2CsC_{70} (sample III) at 350 °C in $Fm\bar{3}m$. (b) Rietveld refinement of Na_2CsC_{70} (sample III) at room temperature in $R\bar{3}m$.

Table 3. Refined Parameters for Na_2CsC_{70} (Sample III) at 350 °C[a]

	x	*y*	*z*	B_{iso}/Å^2	fractional occupancy
C_{70}	0.00	0.00	0.00	0.2(9)	1
Na	0.25	0.25	0.25	30(1)	0.840(4)
Cs	0.5	0.5	0.5	23.7(9)	0.886(6)

[a] $Fm\bar{3}m$ a = 14.983(3), χ^2 = 1.91. R_{wp} = 15.8%, $R(F^2)$ = 9.3%.

lattice parameter of 14.983(3) Å) so refinement was performed in the $Fm\bar{3}m$ space group with sodium and cesium cations on the tetrahedral and octahedral sites, respectively (Figure 5a and Table 3). The refined composition is $Na_{1.680(8)}Cs_{0.886(6)}C_{70}$ and $\chi^2 = 1.91$. It should be noted that the octahedral site displacement parameter compares well with that determined for Rb_3C_{60} at this temperatures,[16] suggesting that the displacement parameters are well determined, although the reduction in occupancy of both cation sites from the target composition by the same factor suggests that the refined composition suffers from site occupancy − displacement parameter correlation due to the limited angular range of the data. The refinements do indicate that a sodium tetrahedral site occupancy of less than one may be possible in fcc C_{70} intercalates.

(16) Bendele, G. M.; Stevens, P. W.; Fischer, J. E. *Europhys. Lett.* **1998**, *41*, 553−558.

Table 4. Refined Parameters for Na_2CsC_{70} (Sample III) at Room Temperature[a]

	x	*y*	*z*	B_{iso}/Å^2	fractional occupancy
C_{70}	0.00	0.00	0.00	2.8(7)	1.000
Na	0.0	0.0	0.223(2)	5(1)	0.54(2)
Cs	0.0	0.0	0.5	12.2(4)	0.883(9)

[a] $R\bar{3}m$ a = 10.443(3) Å, c = 25.706(5) Å. χ^2 = 3.58. R_{wp} = 8.68%, $R(F^2)$ = 8.96%.

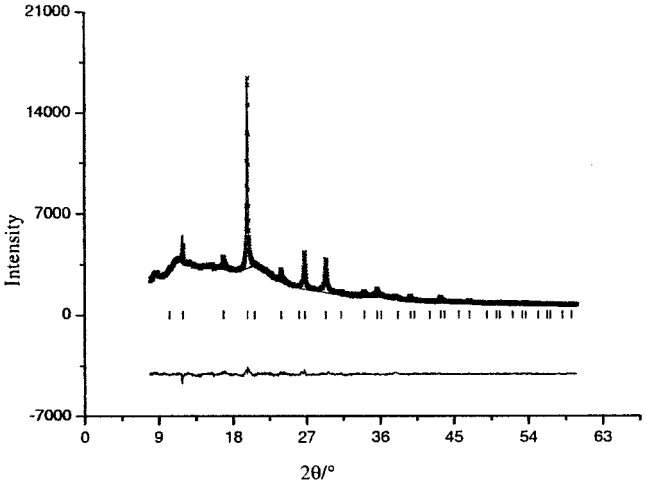

Figure 6. Refinement of Na_2CsC_{70} at 250 °C in $Fm\bar{3}m$. a = 14.890(2) Å. All sites 100% occupied B(C_{70}) = 2 Å^2, B(Cs) = 16.6(3) Å^2, B(Na) = 18(1) Å^2, χ^2 = 1.56, R_{wp} = 2.87%, $R(F^2)$ = 8.05%.

The sample was cooled and data were collected at room temperature. The peakwidth anisotropy (Figure S4b) at room temperature is consistent with lowering of symmetry from cubic to rhombohedral. Le Bail extraction in $R\bar{3}m$ ($\chi^2 = 3.48$) was significantly better than $Fm\bar{3}m$ ($\chi^2 = 4.21$). Although the rhombohedral symmetry implies partial anion orientational ordering, the form factor for an isotropically tumbling C_{70} was used (Figure 5b and Table 4). The sodium deficiency on the tetrahedral site may indicate difficulty in locating all the sodium cations due to disorder, reflected in other samples by large displacement parameters. The metastable nature of this phase is demonstrated by the cell parameters one week after the variable temperature diffraction experiment, as the *c*/*a* ratio has evolved from the initial value of 2.4620(7) to 2.481(2) (a = 10.396(6) Å, c = 25.79(1) Å).

The transition from a broad multiphase/orientationally ordered pattern to a high-temperature cubic phase on heating is confirmed on a fourth sample prepared in an equivalent manner to sample III. The broad fcc-like pattern at room temperature is replaced at 250 °C by a sharp fcc pattern which can be refined with the Na_2CsC_{70} composition with acceptable displacement parameters (Figure 6) − refinement of the sodium site occupancy leads to a value above one due to parameter correlation problems of the type referred to above. The sample-to-sample variability seen in the four Na_2CsC_{70} samples discussed here can be assigned to cation distribution and anion orientation responding to subtle differences in cooling rates.

The susceptibility and peak-to-peak line width derived from the EPR data (Figure S5) on the biphasic/monoclinic (II) and rhombohedral (III) Na_2CsC_{70} samples are shown in Figure 7. In both cases, the temperature dependence of the susceptibility can be fit to $\chi = \chi_0 + C/(T - \theta)$ with identical parameters,

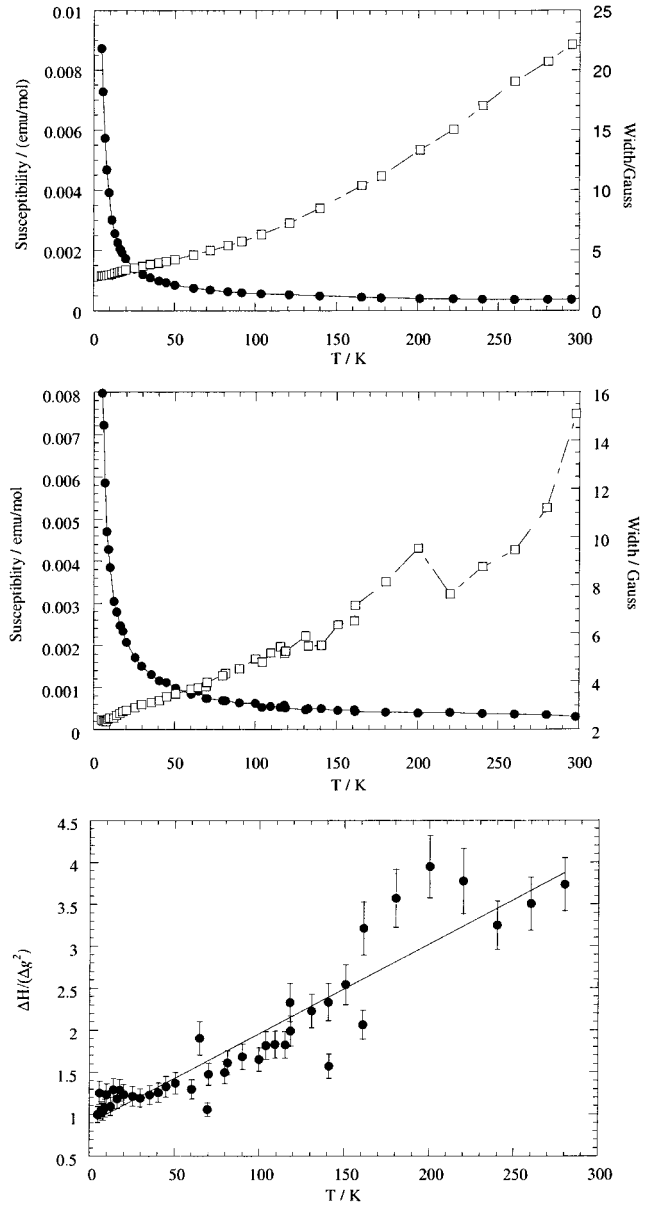

Figure 7. (a) Temperature dependence of the EPR-derived paramagnetic susceptibility (circles) and peak-to-peak line-width (squares) for Na_2CsC_{70} quenched from 600 °C (sample II). (b) Temperature dependence of the EPR-derived paramagnetic susceptibility (circles) and peak-to-peak line width (squares) for Na_2CsC_{70} cooled slowly from 450 °C (sample III). (c) Temperature dependence of $\Delta H_{p-p}/\Delta g^2$ normalized to its low-temperature value for Na_2CsC_{70} (sample III). The errors were calculated assuming the errors in ΔH_{p-p} were negligible. The linear fit to the data is shown.

confirming the conclusions from the structural work concerning the reproducibility of the Na_2CsC_{70} synthesis. The temperature-independent term χ_0 is, in both cases, 2.5×10^{-4} emu mol^{-1}, and the low-temperature Curie tail corresponds to 0.1 unpaired electrons per C_{70} again in both materials, with small Weiss constants of 1.55 K (biphasic/monoclinic) and 0.46 K (rhombohedral). The observation of the same temperature-independent χ_0 term in both biphasic/monoclinic and rhombohedral Na_2CsC_{70} and the temperature dependence of the line width of the EPR signal suggest that both samples are metallic. The *g*-value of 2.0046(1) (Figure S6) is typical of fullerides and its temperature dependence can be used to calculate the conduction electron scattering rate from (2).[17]

$$\Delta H = \frac{1}{\gamma T_1} = \frac{\alpha}{\gamma} \times \frac{\Delta g^2}{\tau} \qquad (2)$$

In a metal above, its Debye temperature the electron−phonon scattering rate $1/\tau$ is proportional to temperature, so $\Delta H/(\Delta g)^2$ should be linear in the temperature (where ΔH is the EPR line width, $\Delta g = g - g_e$ and g_e is the free-electron *g*-value). Due to the proximity of the *g*-value to g_e, the errors on Δg are large at high temperature but a linear relationship can be established at low temperature and be seen to persist into the less well-defined, higher-temperature region (Figure 7c). The nonspin-flip scattering rate $1/\tau$ depends on a proportionality constant, α, which is not well-known in fulleride systems but has been assumed to be $\alpha = 0.005$[18] by analogy with other carbon-based conductors. Using this value, the scattering rate increases from 2×10^{15} to 8×10^{15} s^{-1} over the whole temperature range and changes linearly with temperature below 150 K, consistent with a metallic system in which the dominant conduction electron scattering mechanism is the electron−phonon interaction.[18] The time between electron−phonon scattering events is thus of the same order of magnitude as obtained for K_3C_{60}, Rb_3C_{60}, and Na_2CsC_{60}.[18] The physically reasonable values and consistency with other metallic fullerides supports the assignment of metallic behavior to these Na_2CsC_{70} phases. Between 150 and 240 K there is a clear deviation from this linear behavior which may signal an orientational ordering transition. The magnitude and temperature dependence of the line width is different for each sample. The line width of the predominantly rhombohedral material is smaller, suggesting that the conduction electron spin lifetime is longer than in the biphasic/monoclinic material. The temperature independent component of the susceptibility is attributed to the Pauli paramagnetism of a metallic phase and has the same value for both samples, yielding a density of states at the Fermi energy, $N(E_f)$, of 4.02 states/eV/C_{70}/spin. The low-field SQUID magnetization measurements indicated that the Na_2CsC_{70} samples were not superconducting above 1.5 K.

^{13}C MAS NMR data on Na_2CsC_{70} (cooled at 0.01 °C min^{-1} from 450 °C) at room temperature and 230 °C are shown in Figure 8, acquired at a spinning speed of 6 kHz. The dramatic sharpening of the spectrum on heating from room temperature to 230 °C is due to the removal of the chemical shift anisotropy (CSA) by motional narrowing, with five separate lines visible between 18 and 234 ppm. This is consistent with the transition to fcc symmetry in this temperature range seen in the variable temperature diffraction experiments. The relative intensities of the lines are a function of the spinning speed (Figure S7) which demonstrates that the CSA is at least 5 kHz even at 230 °C and is not completely removed by MAS, making assignment of resonances to individual carbon atoms difficult. The average paramagnetic shift of the ^{13}C resonances is independent of temperature consistent with the metallic behavior deduced from the EPR data.

The Raman spectrum of the rhombohedral sample III prepared during the variable temperature diffraction experiment was measured at room temperature and is presented in Figure S8 together with the spectrum of pristine C_{70}. The large number of overlapping Raman active modes makes fitting the spectrum

(17) Elliott, R. J. *Phys. Rev.* **1954**, *96*, 266−287.
(18) Petit, P.; Robert, J.; Yildrim, T.; Fischer, J. E. *Phys. Rev. B* **1996**, *54*, R3764−R3767.

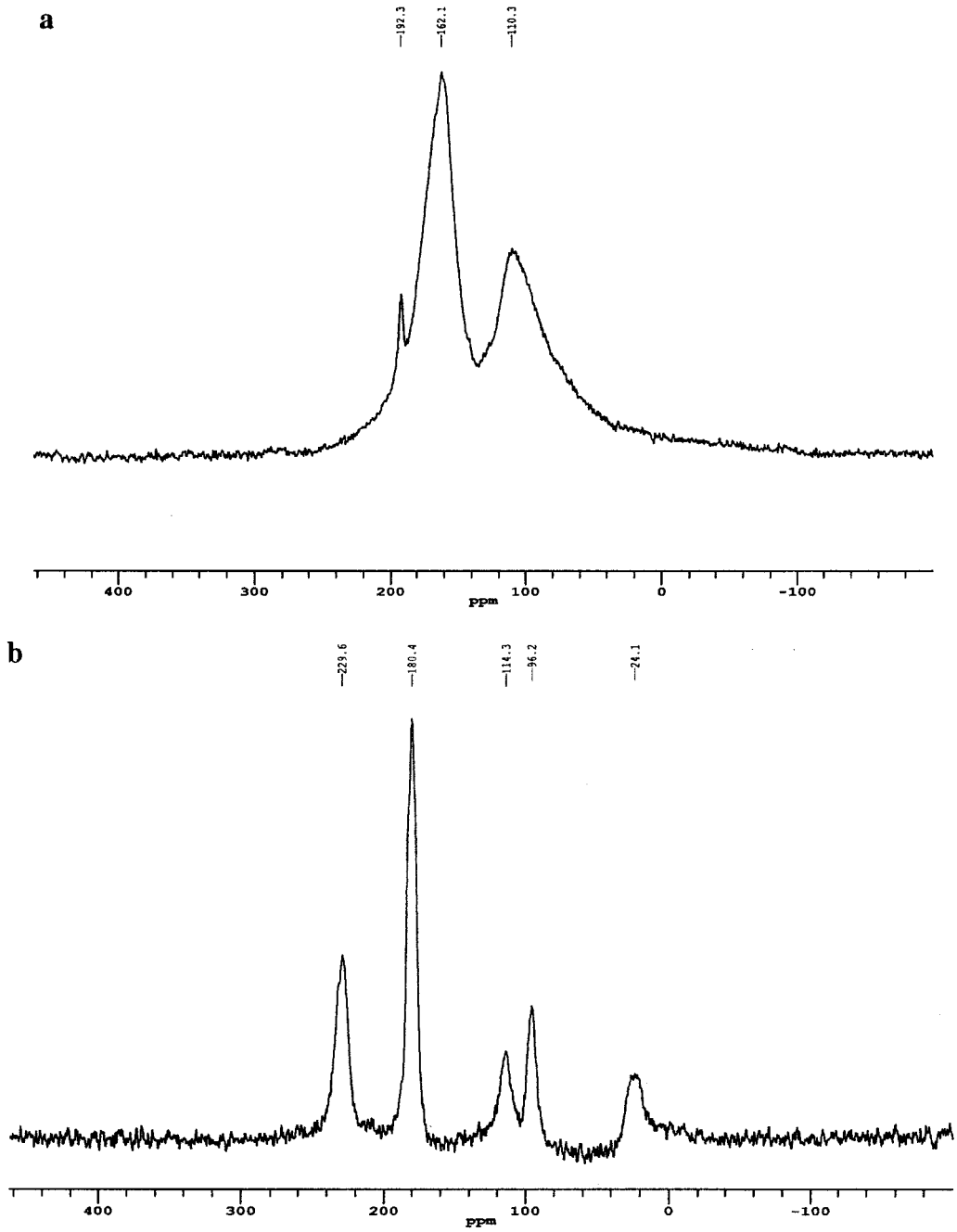

Figure 8. (a) Room temperature ^{13}C MAS NMR spectrum of Na_2CsC_{70}, using a 6 kHz spinning speed. (b) ^{13}C MAS NMR spectrum of Na_2CsC_{70} at 230 °C (6 kHz).

to obtain peak positions and peak widths a difficult task, accomplished for K_xC_{70}[8] and A_6C_{70} (A = K, Rb, Cs).[19] All the Raman-active modes in C_{70} appear in the Raman spectrum of Na_2CsC_{70}, in contrast to the loss of the H_g modes from the Raman spectrum of K_3C_{60} due to broadening induced by electron−phonon coupling. The Raman spectrum of metallic K_4C_{70} displays all the Raman-active modes. An estimate of the dimensionless electron−phonon coupling constant can be made by fitting the peaks in the spectrum and using (3)[8,20] for λ, the electron−phonon coupling constant,

$$\lambda = \frac{1}{\pi N(E_f)} \sum_i \frac{\Delta\Gamma_i}{\hbar\omega_i^2} \qquad (3)$$

where ω_i is the frequency of mode i, $\Delta\Gamma_i$ is the difference in FWHM of mode in Na_2CsC_{70} and mode i in pristine C_{70}, and $N(E_f)$ is taken as the value determined by EPR. The sum is over all optical branches at wavevector $q = 0$. There are 53 Raman-allowed modes for C_{70} corresponding to the symmetry species $12A_1' + 22E_2' + 19E_1''$. Fitting of the data in Figure S8 requires the use of 52 pseudo-Voigt functions. The width of the C_{70} lines was assumed to be constant for all modes and was determined by fitting the C_{70} Raman data. The resulting estimate for the electron−phonon coupling constant was λ = 2.6 which is four times larger than the value estimated for

(19) Wang, K.-A.; Zhou, P.; Rao, A. M.; Eklund, P. C.; Jishi, R. A.; Dresselhaus, M. S. *Phys. Rev. B* **1993**, *48*, 3501−3506.
(20) Zhou, P.; Wang, K.; Eklund, P. C.; Dresselhaus, G.; Dresselhaus, M. S. *Phys. Rev. B* **1993**, *48*, 8412−8417.

Table 5. Refined Cation Parameters for K_2CsC_{70} at 350 °C[a]

	x	*y*	*z*	B_{iso}/Å^2	fractional occupancy
C_{70}	0.00	0.00	0.00	2.48(48)	1.000
K	0.25	0.25	0.25	18.8(7)	1.040(14)
Cs	0.5	0.5	0.5	22.6(4)	1.022(6)

[a] $Fm\bar{3}m$ $a = 15.2342(2)$ Å. $\chi^2 = 1.87$. $R_{wp} = 5.32\%$, $R(F^2) = 5.2\%$.

K_3C_{60}[20] of $\lambda = 0.6$. This is a strong indicator that inhomogeneous line broadening is producing overestimates for the intrinsic line widths of the modes. Such inhomogeneous broadening is consistent with the quenched cation positional and anion orientational disorder indicated by the Rietveld refinements.

K_2CsC_{70}. The final heat treatment adopted for this composition was 450 °C for 3 days followed by cooling to room temperature at 0.01 °C per min. The resulting room-temperature powder diffraction pattern (Figure S9) is quite different from that found for any of the Na_2CsC_{70} samples and cannot be indexed as a single fcc − related phase. Temperature-dependent diffraction data over the range of the fcc 311 reflection ($11.5 < 2\theta/° < 14.5$) were collected in 5° increments between room temperature and 200 °C. A single reflection coalesces from the multiple reflections at 195 °C (Figure 9a). Data collected on cooling from 200 °C indicate that the resulting high-symmetry phase can be supercooled to 155 °C before disproportionating into the original multiphase pattern (Figure S10). A high quality data set in the high-symmetry region was collected at 350 °C and Le Bail extraction indicated that the material was metrically cubic ($a = 15.235(1)$ Å, $\chi^2 = 2.19$). Rietveld refinement using the orientationally disordered C_{70} form factor and a cation site-ordered model with potassium and cesium cations occupying the tetrahedral and octahedral sites respectively converged smoothly to $\chi^2 = 1.87$ (Figure 9b, Table 5). The refined composition is $K_{2.08(3)}Cs_{1.022(6)}C_{70}$, which corresponds very well to the target composition. The displacement parameters are comparable to those refined for Na_2CsC_{70} indicating that the previously refined compositions for these phases should be reliable. Taken together with the ^{13}C MAS NMR spectra in the following section, the diffraction data provide good evidence for a single cubic K_2CsC_{70} phase above 200 °C whose temperature dependence is considerably different from the cubic and rhombohedral phases of Na_2CsC_{70}.

^{13}C MAS NMR data from K_2CsC_{70} (spinning at 3.5 kHz) between room temperature and 250 °C are shown in Figure 10. The disappearance of the feature at 152.4 ppm as the temperature is raised from 150 to 200 °C provides strong evidence for the formation of a single-phase sample from a two-phase sample between these temperatures. Comparison between the ^{13}C MAS NMR spectra of Na_2CsC_{70} at room temperature and K_2CsC_{70} at 200 °C reveals a similarity in the line shape of the spectra but a considerable difference in their line widths. The implication is that although the crystal structures of the two phases are similar, the molecular reorientation processes occur at very different rates in the two spectra. This is hardly surprising considering the difference in temperature at which the two spectra were acquired. In K_2CsC_{70} at 200 °C, the thermal energy is sufficient to cause rapid reorientation between symmetry equivalent orientations of the C_{70} molecule compared to those in Na_2CsC_{70} at room temperature. The high-temperature K_2CsC_{70} spectrum therefore confirms that at room temperature the sample of Na_2CsC_{70} studied by NMR is a C_{70}^{3-} salt.

Na_2C_{70}. Samples were prepared as for Na_2CsC_{70} with a final temperature of 450 °C and cooling at 0.01 °C per min. The room-temperature diffraction pattern of the material cooled at 0.16 °C min^{-1} from 450 °C (Figure S11) cannot be indexed as a single phase. Cooling at 0.01 °C per min results in a two-phase mixture in which the predominant phase is rhombohedral with cell parameters approaching those of C_{70} at room temperature and a tetrahedral sodium site occupancy which refines to zero, suggesting disproportionation into C_{70} and a sodium-rich phase. Variable temperature diffraction data collected on this composition, unlike those measured for K_2CsC_{70} and Na_2CsC_{70}, were completely reversible. High quality data collected at 250 °C could not be indexed with the cubic/rhombohedral two-phase model found for Na_2CsC_{70} − the symmetry of the second phase needed to be trigonal rather than rhombohedral to index the patterns, giving a mixture of $Fm\bar{3}m$ C_{70} and a new $P\bar{3}m1$ ($a = 10.617(1)$ Å, $c = 25.998(5)$ Å) Na_xC_{70} phase. As the second phase is sodium-rich and present in only ∼25% mole fraction, a definitive structural model cannot be deduced but refinement of the occupancies of atomic positions generated assuming a cubic sodium cluster occupies the octahedral voids in the $P\bar{3}m1$ phase generates an $Na_{7.7(2)}C_{70}$ phase with the fit shown in Figure S12 and a phase fraction of 27.2%, yielding an overall composition of $Na_{2.2(1)}C_{70}$ in good agreement with the expected value based on the starting composition. The two-phase nature of the material and the presence of C_{70} as one of these phases was confirmed by ^{13}C MAS NMR measurements with differing recycle delays. Measurement with a recycle delay of 1 min gives a spectrum dominated by the five inequivalent atom C_{70} resonances (Figure S13a), while the shorter pulse separation of 1 s saturates the pure C_{70} resonances and produces a quite different spectrum characteristic of the more rapidly relaxing second sodium fulleride phase (Figure S13b). Spectra collected on heating (Figure S14) reveal the spinning sidebands disappear at 100 °C due to enhanced molecular motion to afford a spectrum characteristic of the Na_yC_{70} phase, while above this temperature the pristine C_{70} resonances become more dominant due to the enhanced molecular motion and shortened relaxation time. This demonstrates, consistent with the refined synchrotron X-ray data, that pristine C_{70} is present at all temperatures up to 225 °C and that Na_2C_{70} is not thermodynamically stable. All the changes in the NMR spectra with temperature are completely reversible.

Discussion

The A_3C_{70} composition does not have the stability found for A_3C_{60}, demonstrated by the wide range of A_3C_{60} fullerides and the difficulty in preparing even simple binary A_3C_{70} phases at room temperature. All the fcc interstitial sites must be singly occupied to attain this composition, and the feasibility of this for a particular fullerene can be quantitatively assessed using simple spherical shell estimates of the interstitial site sizes. Na_2CsC_{70} is accessible because both the sodium and cesium cations are size-matched to the sites they occupy when the fulleride anion is orientationally disordered and thus occupying its maximum time-averaged volume, although parameter correlation effects do not allow us to exclude reduced Na occupancy of the tetrahedral site. K_2CsC_{70} is unstable to phase separation at room temperature but exists as a stable cubic phase above 195 °C. This is because the thermal expansion of the close-packed C_{70}^{3-} lattice enhances the tetrahedral site radius from

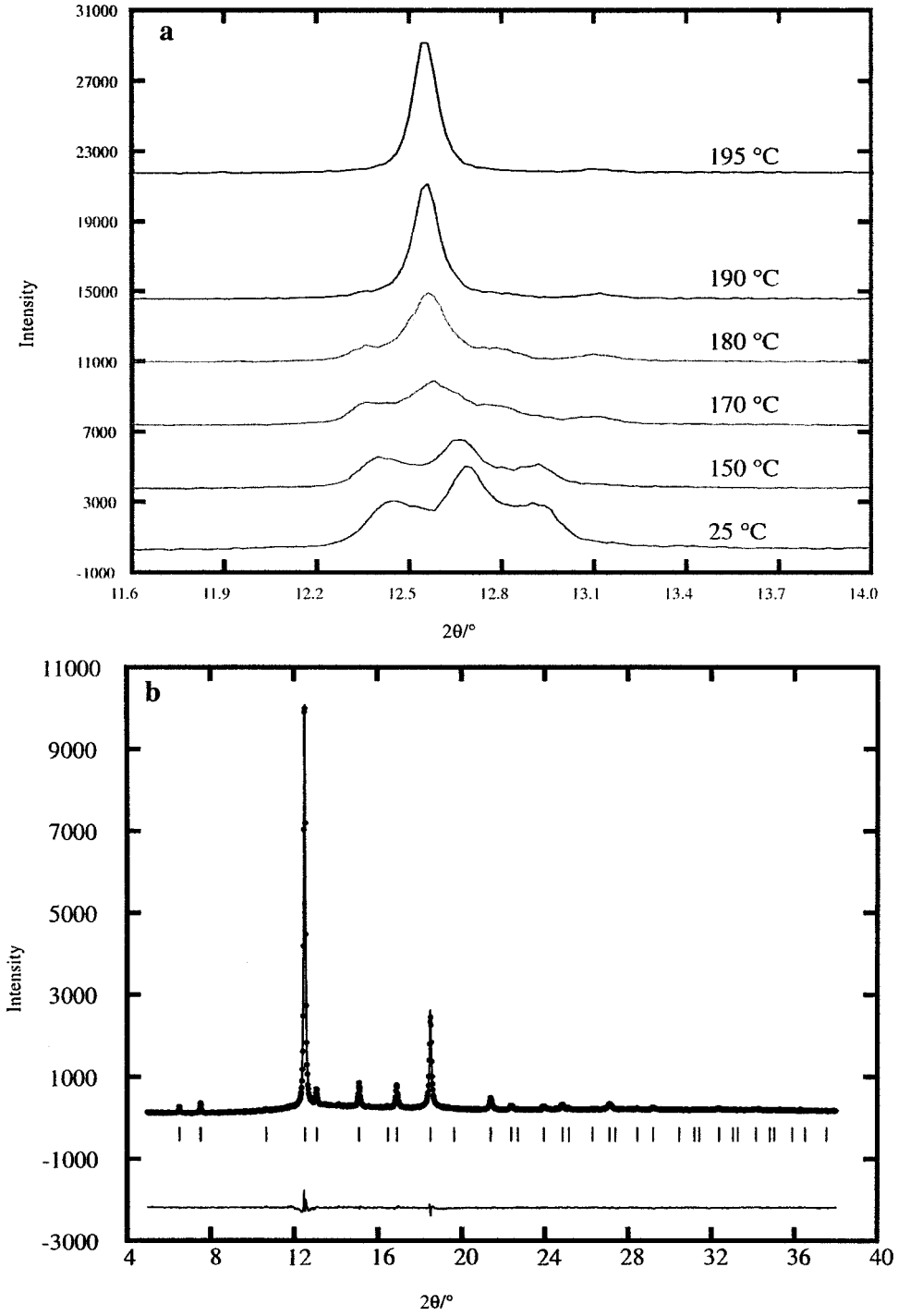

Figure 9. (a) Evolution of the main diffraction feature of K_2CsC_{70} (which becomes the 311 reflection in the high-temperature $Fm\bar{3}m$ phase) with increasing temperature. (b) Rietveld refinement of K_2CsC_{70} at 350 °C using a single phase $Fm\bar{3}m$ model with parameters given in Table 5.

1.18 to 1.23 Å, sufficiently close to the K^+ ionic radius to allow this cation to occupy the tetrahedral site in an fcc array of isotropically reorienting C_{70}^{3-} anions. As in the case of A_3C_{60}, isotropic reorientation and spherical disorder are not equivalent − partial orientational order of the anions can allow the interstitial cations to nest into the faces of the anions and occupy sites that appear too small based on spherical shell estimates. The strict site ordering of the K^+ and Cs^+ cations in this phase even at 350 °C is clear evidence for the importance of size-matching, as is the 440 K reported lower stability limit of K_3C_{70}: if thermally driven matching of the tetrahedral site size to that of the cation occupying it determines the stability of A_3C_{70} phases, then the identity of the octahedral cation (K^+ or Cs^+) should not control the phase stability, as is observed. (K_2CsC_{70} forms on heating at 468 K.)

The cation site ordering in K_2CsC_{70} and Na_2CsC_{70} appears as complete as it is in analogous A_2CsC_{60} phases. The size-matching criteria for the stability of A_xC_{70} salts appear more stringent than for the corresponding A_xC_{60} materials, and this can be ascribed to the enhanced size of the interstitial sites. The nonexistence of the Na_2C_{70} phase demonstrates this, indicating that, despite the good size-matching on the tetrahedral

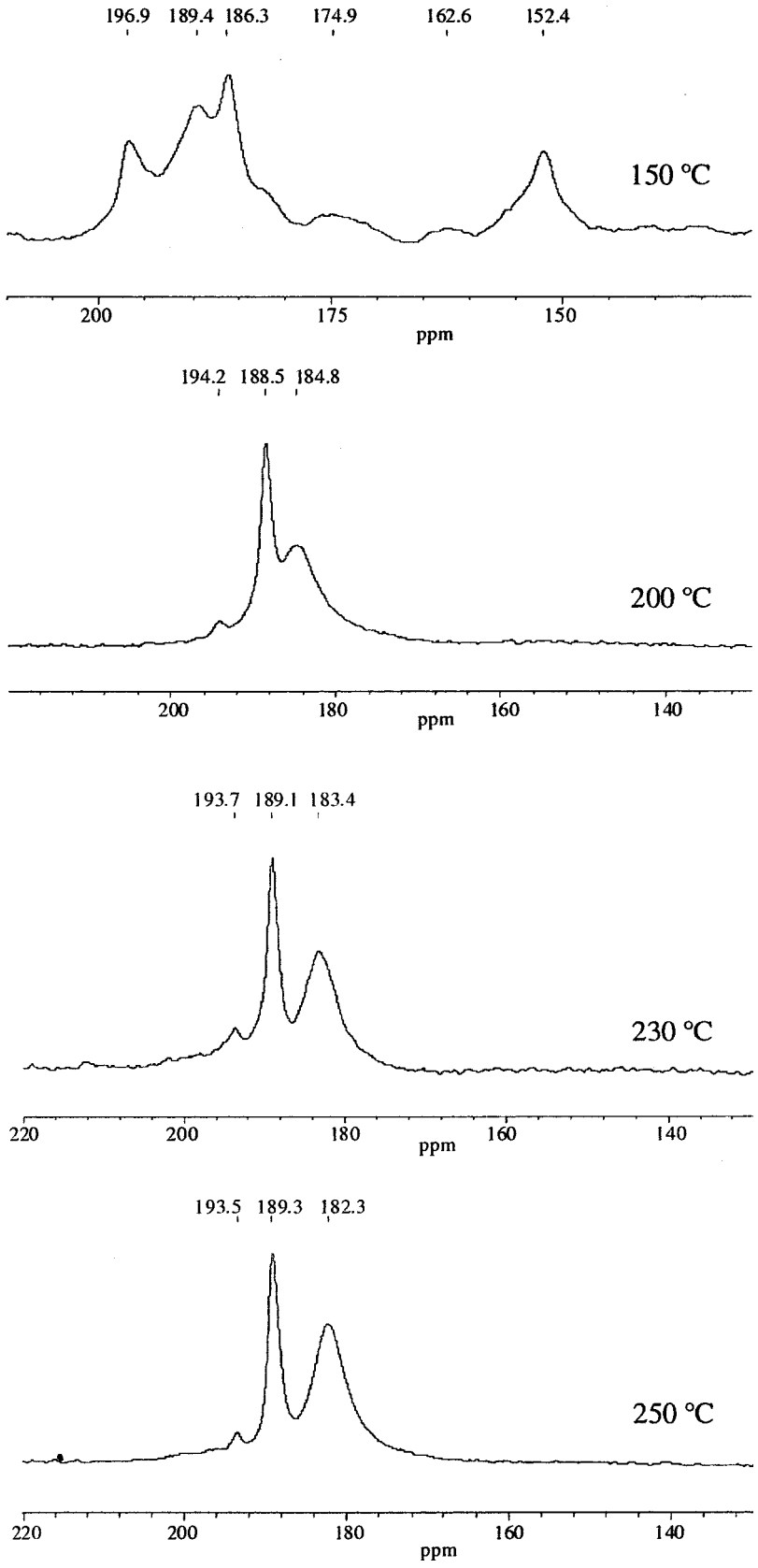

Figure 10. Evolution of the ^{13}C MAS NMR spectrum of K_2CsC_{70} with temperature.

sites, occupation of the large octahedral site in the fcc C_{70} array is required for the stability of this array in intercalation compounds − the second phase present with pristine C_{70} at the multiphase Na_2C_{70} composition has multiple occupancy of the large octahedral sites as in Na_xC_{60}[21,22] and Ca_xC_{60},[23] in contrast to Na_2C_{60}, where the smaller octahedral sites are vacant. The stability of such multication units on the octahedral site in C_{70} intercalates may be a dominant feature of the structural

chemistry of sodium in C_{70} and account for the tetrahedral sodium deficiency observed in Na_2CsC_{70} (sample III) at room temperature.

The correlation between the stability of the fcc C_{70} array, the cation site occupancy, and the anion reorientational dynamics is clear from the variable temperature X-ray and NMR data, and the effect of cooling rate on the ambient temperature structure of Na_2CsC_{70}. The interplay between the dynamics of the ellipsoidal C_{70} molecule and the fcc sphere packing within which it is placed give pristine C_{70} a complex structural phase diagram.[12] The cubic phase, observed at above 300 K, transforms on cooling to an intermediate rhombohedral phase due to the freezing of molecular rotations about the short ellipsoid axes while maintaining dynamical disorder about the molecular five-fold axis. This leads to a structure in which the five-fold axes are preferentially aligned along one of the <111> direction cube body diagonals. Further cooling produces a monoclinic cell, in which the fulleride anions can be fully orientationally ordered as the space group contains no higher symmetry elements above the two-fold axis and mirror plane of the C_{70} molecule. This dynamical reorientation of the anions appears to be hindered by the introduction of cations to the interstitial sites in the fcc array, as the ^{13}C chemical shift anisotropy appears much larger in both Na_2CsC_{70} and K_2CsC_{70} than in pristine C_{70},[24] and considerably higher temperatures are required for the onset of isotropic reorientation to form the fcc phase, with associated motional narrowing in the ^{13}C MAS NMR spectra. At room temperature, orientational order may be complete (monoclinic symmetry, sample II) or partial (rhombohedral, sample III), with the cooling protocol strongly influencing the outcome in a way that proved hard to control. It is noticeable that the slower the cooling rate, the further the rhombohedral c/a ratio deviates from the ideal cubic value of $\sqrt{6}$. The evolution of the c/a ratio with time at room temperature indicates the metastable nature of the anion orientations afforded by the cooling procedures adopted here. Since the space group symmetry in all the samples at room temperature clearly indicates at least partial orientational ordering, the refined parameters from those models, where the C_{70}^{3-} anions are assumed to be isotropic shells of charge, should be treated with caution. The spread of rhombohedral cell parameters observed due to the different thermal treatments and resulting quenched anion orderings are equivalent to variation of a pseudo-fcc cell parameter between 14.75 and 14.80 Å, indicating that the interfulleride separation in the A_3C_{70} systems can be tuned.

Theory predicts that the metallic ground state should be favored by orientational anion disorder for C_{70} fullerides.[25] The temperature-independent susceptibility and the physically reasonable conduction electron-scattering rate derived from the EPR line width and the temperature independence of the paramagnetic shift in the ^{13}C nuclear magnetic resonance signal all indicate the Na_2CsC_{70} samples are metallic, but have a density of states at the Fermi energy of only 42% of that found for K_3C_{60}. This may be a result of conduction band broadening produced by the structural disorder. The pronounced density-of-states reduction can be shown using simple weak-coupling BCS or McMillan expressions[26] for T_c to reduce the predicted superconducting transition temperature of Na_2CsC_{70} to below 0.1 K. The dominant effect of $N(E_f)$ on T_c is entirely consistent with the metallic behavior and absence of superconductivity seen here. As the fulleride point symmetries and diffraction patterns are inconsistent with anion orientational order, the partial disorder will broaden the density of states in the (LUMO + 1) band and reduce $N(E_f)$ compared with the A_3C_{60} systems, where there is less anion orientational disorder. This is accentuated by the 3^- charge no longer corresponding to a peak in the $N(E)$ function because it is not a half-filled configuration, due to the different frontier orbital degeneracies of C_{60} and C_{70}.

The C_{70}^{3-} anion charge corresponds to 25% filling of the (LUMO + 1) band. The property measurements on the Na_2CsC_{70} phases studied here are consistent with this band-filling giving metallic but not superconducting behavior. This contrasts with superconductivity observed at the C_{70}^{4-} charge and a half-filled (LUMO + 1) band in field-effect transistors.[11] The distinguishing features between these two cases are the band filling and the extent of quenched anion positional disorder in the A_3C_{70} phases. In C_{60} − based superconductors, deviations of over 0.5 electrons either side of half-filling the t_{1u} band totally quench superconductivity.[27,28] The present results are entirely consistent with this view of electronic control of fulleride superconductivity, although the influence of the anion disorder on broadening the (LUMO + 1) − derived bands and thus lowering the density of states at the Fermi level should not be neglected.

In summary, although the preparation of a metallic rhombohedral C_{70}^{3-} salt, in which the long axes of the ellipsoidal anions are aligned with the cubic [111] direction, has been achieved by using a judicious choice of alkali metal cations, the low density of states at the Fermi energy prevent superconductivity. This problem appears to be intrinsic to doped C_{70} systems due to the structural disorder induced by the ellipsoidal shape of the molecule when intoduced into high-symmetry sphere packings such as fcc, which is quenched on cooling by interference with reorientational dynamics from the intercalated cations. The absence of superconductivity in these C_{70}^{3-} systems is consistent with the idea that superconductivity in fulleride systems is strongly controlled by the requirement for the Fermi level to correspond to a half-filled band.

Acknowledgment. We thank the U.K. EPSRC for support under GR/M04006 and a studentship to M.S.D., and the Leverhulme Trust for grant F/25/BX. This work was partly supported by the Grant-in-Aid by the Ministry of Education, Science and Culture of Japan. We thank Dr. A. N. Fitch and Dr. M. A. Roberts for their assistance with the BM16 and 9.1 diffractometers.

Supporting Information Available: Supplementary figures (PDF). This material is available free of charge via the Internet at http://pubs.acs.org.

JA017780B

(21) Rosseinsky, M. J.; Murphy, D. W.; Fleming, R. M.; Tycko, R.; Ramirez, A. P.; Siegrist, T.; Dabbagh, G.; Barrett, S. E. *Nature* **1992**, *356*, 416−418.
(22) Yildirim, T.; Zhou, O.; Fischer, J. E.; Bykovetz, N.; Strongin, R. A.; Cichy, M. A.; III, A. B. S.; Lin, C. L.; Jelinek, R. *Nature* **1992**, *360*, 569.
(23) Kortan, A. R.; Kopylov, N.; Glarum, S.; Gyorgy, E. M.; Ramirez, A. P.; Thiel, F. A.; Haddon, R. C. *Nature* **1992**, *355*, 529−532.
(24) Tycko, R.; Dabbagh, G.; Vaughan, G. B. M.; Heiney, P. A.; Strongin, R. M.; Cichy, M. A.; Smith, A. B., III. *J. Chem. Phys.* **1993**, *99*, 7554−7564.
(25) Lu, J. P.; Gelfand, M. P. *Phys. Rev. B* **1995**, *51*, 16615−16618.
(26) McMillan, W. L. *Phys. Rev.* **1968**, *167*, 331.
(27) Yildirim, T.; Barbedette, L.; Fischer, J. E.; Lin, C. L.; Robert, J.; Petit, P.; Palstra, T. T. M. *Phys. Rev. Lett.* **1996**, *77*, 167−170.
(28) Kosaka, M.; Tanigaki, K.; Prassides, K.; Margadonna, S.; Lappas, A.; Brown, C. M.; Fitch, A. N. *Phys. Rev. B* **1999**, *59*, R6628−R6630.